

Bias Characterization of FengYun-4A AGRI Infrared Channels Using Advanced Radiative Transfer Modeling System (ARMS)



Fei Tang¹, Fuzhong Weng² and Xiaoyong Zhuge¹

1、Nanjing Joint Institute for Atmospheric Sciences

2、Chinese Academy of Meteorological Sciences

Email: tangf@cma.gov.cn

The 23th International TOVS Study Conferences
28 June 2021



outline

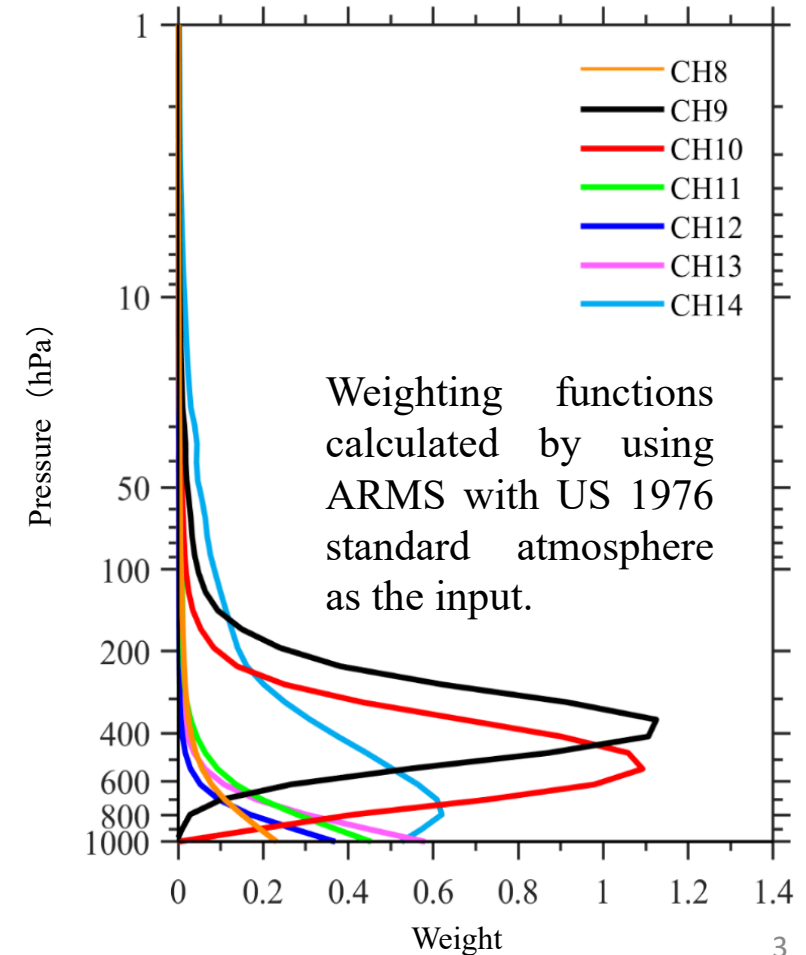
- Description of FengYun-4A/AGRI and ARMS
- Data and Method
- AGRI Bias Characteristics
- Simulation Difference between ARMS and RTTOV
- Conclusions

Characteristics of FengYun-4A/AGRI

Bands

- The FengYun-4A satellite was launched in 2016. It is located at 35,786 km above the equator at 104.7°E.
- Advanced Geosynchronous Radiation Imager (AGRI) onboard FengYun-4A satellite has a total of 14 bands. It provides a full-disk observation with an interval of 15 minutes.
- Bands 8, 11, 12 and 13 are surface-sensitive. Bands 9 and 10 are located in a water vapor absorption band with their peak weighting located at 350 hPa and 500 hPa, respectively. Band 14 is located in a carbon dioxide absorption band.

	Channel No.	Central wavelength (μm)	Spectral interval (μm)	SNR or NEDT specified (km)	Spatial resolution at SSP (km)
Visible	1	0.47	0.45-0.49	200@100%albedo	1
	2	0.65	0.55-0.75	200@100%albedo	0.5
	3	0.825	0.75-0.90	200@100%albedo	1
Near-infrared	4	1.375	1.36-1.39	200@100%albedo	2
	5	1.61	1.58-1.64	200@100%albedo	2
	6	2.25	2.1-2.35	200@100%albedo	2
	7	3.75	3.5-4.0	0.7 K @300 K	2
8	0.2 K @ 300 K			4	
Infrared	9	6.25	5.8-6.7	0.3 K @ 260 K	4
	10	7.1	6.9-7.3	0.3 K @ 260 K	4
	11	8.5	8.0-9.0	0.2 K @ 300 K	4
	12	10.7	10.3-11.1	0.2 K @ 300 K	4
	13	12.0	11.5-12.5	0.2 K @ 300 K	4
	14	13.5	13.2-13.8	0.2 K @ 300 K	4



Research Status of AGRI Bias Characteristics

Three studies have contributed to AGRI bias assessment using radiative transfer model:

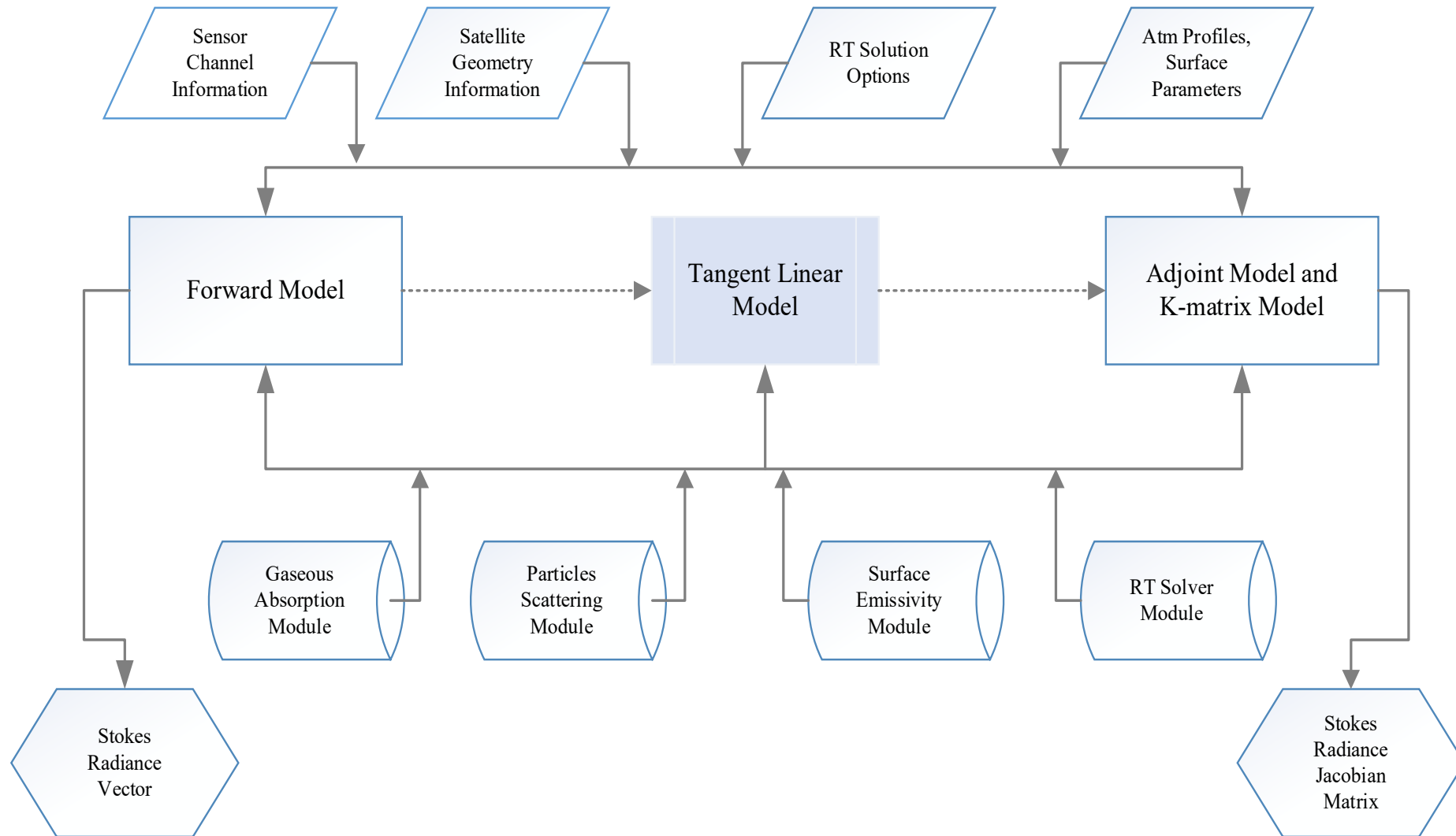
- 1) Qu et al. (2019) used the ECMWF Reanalysis-5 (ERA5) data as input to the **RTTOV** model to calculate and analyze the biases of the AGRI seven 4-km-resolution IR bands.
- 2) Geng et al. (2020) also employed the **RTTOV**, but they used Global Forecast System (GFS) analysis data as input.
- 3) Zhu et al. (2020) coupled the **RTTOV** and ERA5 to evaluate the AGRI IR bands bias over its full-disk.

The Advanced Radiative Transfer Modeling System (ARMS) has been developed in China Meteorological Administration to support FengYun satellite missions.

This research aims to use the new developed **ARMS** to characterize the infrared band biases of AGRI onboard FengYun-4A satellite.

Two different NWP background fields (ERA5 and NCEP FNL) are used as a comparison of the model simulation.

Advanced Radiative Transfer Modeling System (ARMS)



Main Features of ARMS

- ❑ There are four solvers in ARMS: polarimetric two-stream approximation (**P2S**), vector doubling adding (**VDA**), hybrid radiative transfer scheme (**HRTS**) and advanced doubling adding (**ADA**).
- ❑ P2S and HRTS are recommended as the preferred solvers to simulate the Stokes vector and scalar intensity, respectively.
- ❑ For the particle absorption and scattering, **a super-spheroidal model is implemented** in ARMS. It has the advantage of generating a lookup table for the fast calculation of aerosols.
- ❑ Six hydrometeors (e.g., **cloud, rain water, cloud ice, snow, graupel and hail**) can be considered in ARMS.

outline

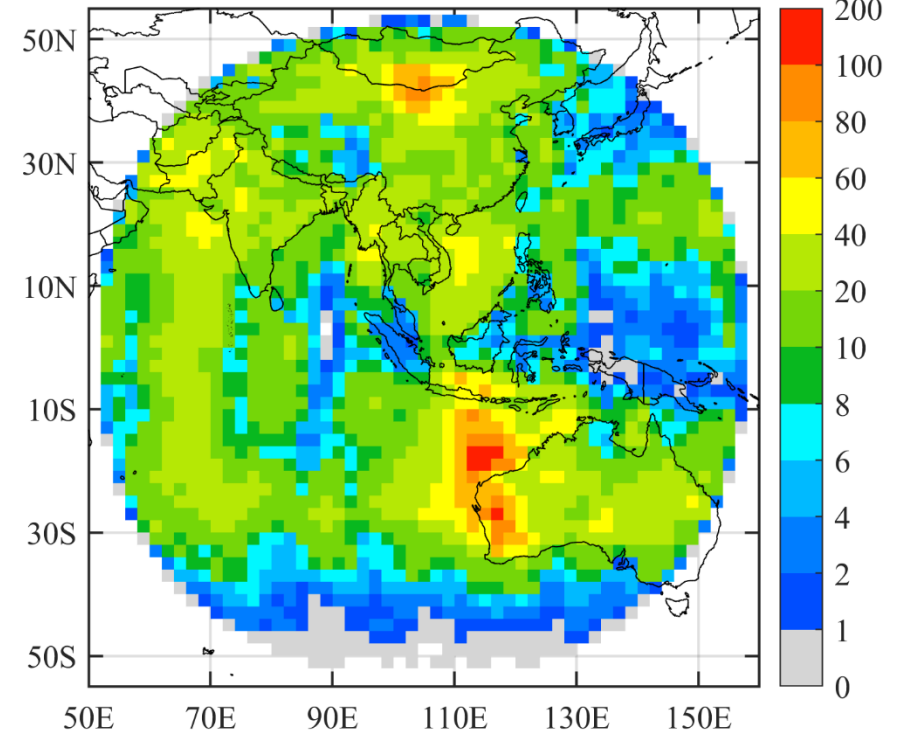
- Description of FengYun-4A/AGRI and ARMS
- **Data and Method**
- AGRI Bias Characteristics
- Simulation Difference between ARMS and RTTOV
- Conclusions

Data and Method

Data used in this study

- **AGRI: bands 8-14 L1 brightness temperature**
 - scan lines × scan pixels: 2748×2748
 - spatial resolution: 4 km
 - full disk with satellite zenith angle < 60°
 - **MODIS cloud mask product: L2A MOD/MYD35**
 - four types: clear, probably clear, probably cloudy and cloud
 - spatial resolution: 1 km
 - **NWP data: ECMWF ERA5 and NCEP FNL (FNL)**
 - four hours: 00,06, 12 and 18 UTC
 - 0.25°×0.25° spatial resolution
- Only AGRI clear-sky observations in January, April, July and October, 2019, are considered.

Spatial distribution of AGRI clear-sky data counts within 2°×2° box. ($\times 10^3$)



Method

Step 1: Data from Aqua or Terra satellite passing over the AGRI full disk observation area within 15 minutes are matched to AGRI observation pixels. Only AGRI pixel within its 4 km-FOV are all MOD35/MYD35 clear pixels is retained.

Step 2: AGRI clear-sky observations are simulated using ARMS .
—surface emissivity model: Wu and Smith (1997) (ocean); Camel_HSRemis (land).

Step 3: Calculate mean bias of AGRI infrared bands and analyze it.

outline

- Description of FengYun-4A/AGRI and ARMS
- Data and Method
- **AGRI Bias Characteristics**
- Simulation Difference between ARMS and RTTOV
- Conclusions

Anomalies of AGRI Brightness Temperature at band

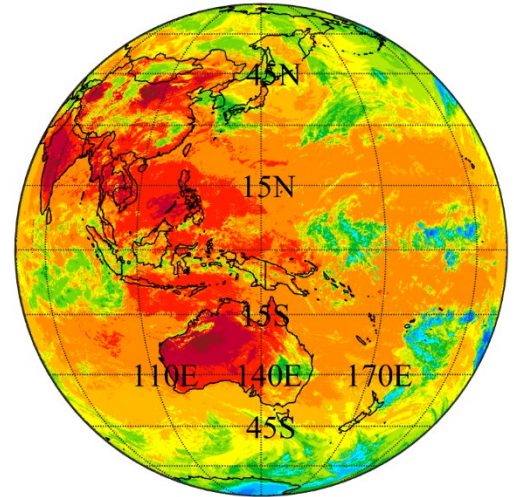
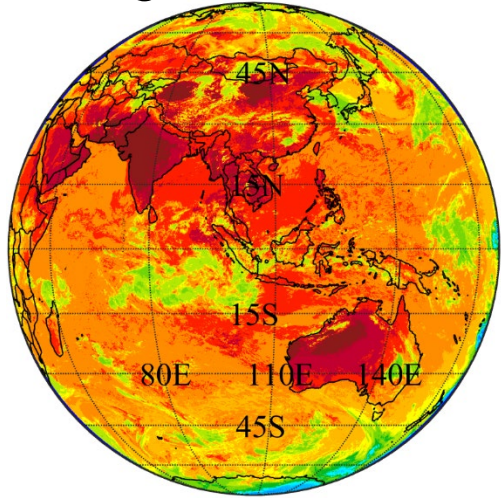
8

FengYun-4A/AGRI

Himawari-8/AHI

23 April, 2019

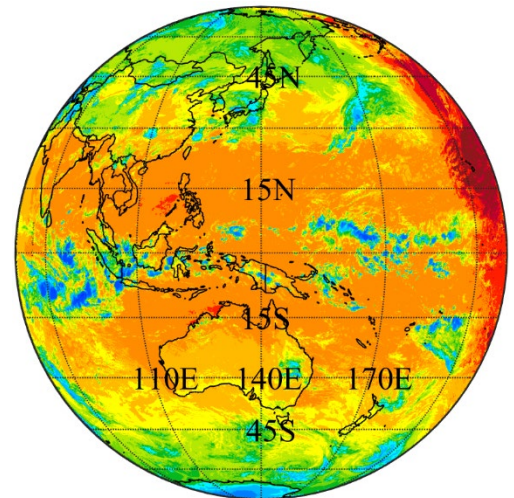
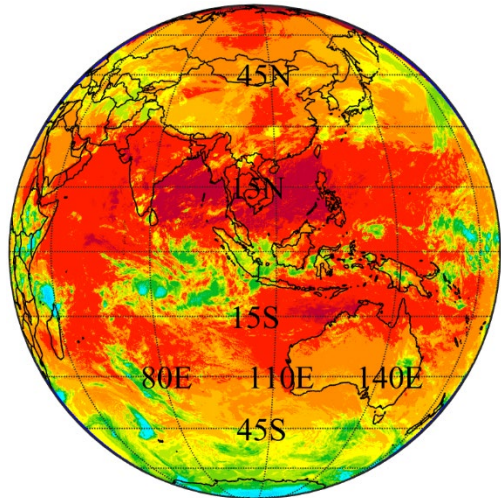
0600 UTC →



Daytime

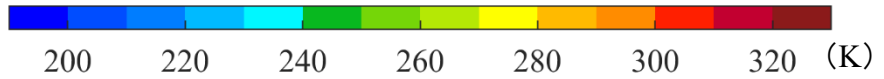
The AGRI and AHI brightness temperatures in the overlapping region agree well except the clouds where AGRI brightness temperatures are slightly higher than those of AHI.

1700 UTC →

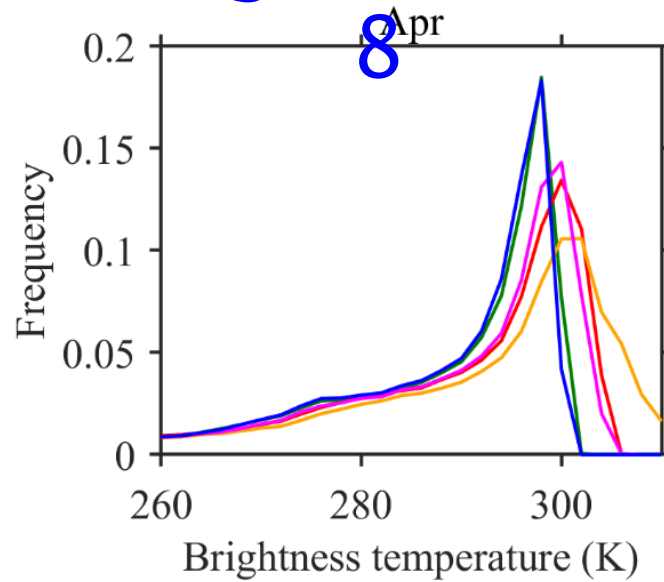
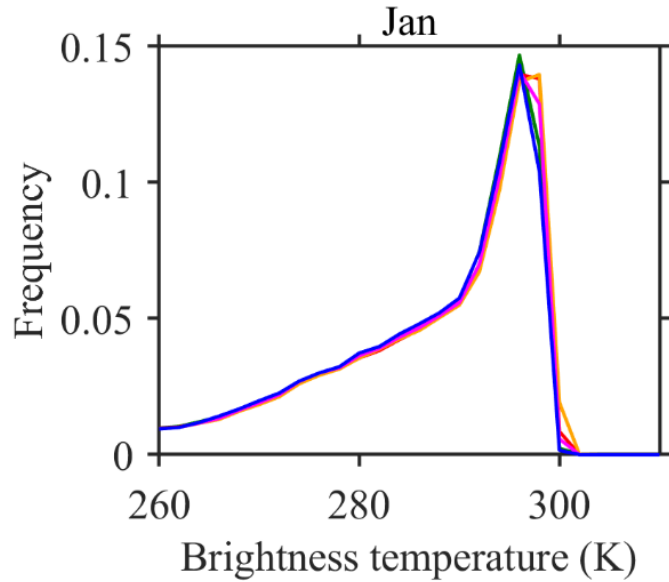


Midnight

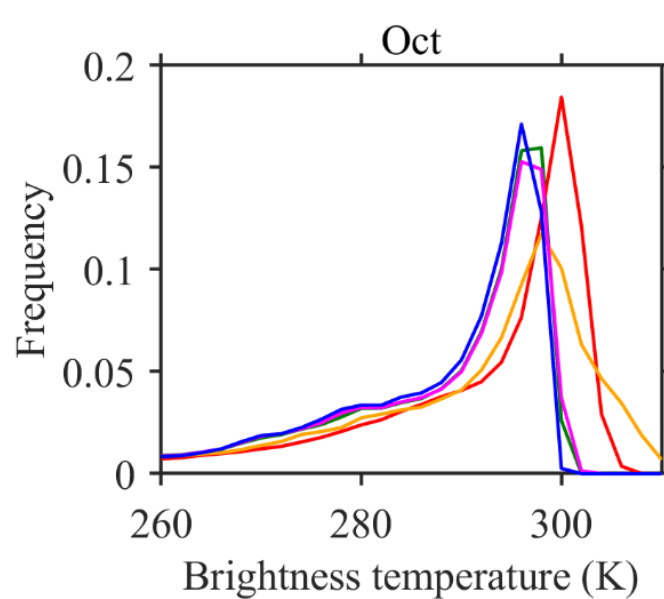
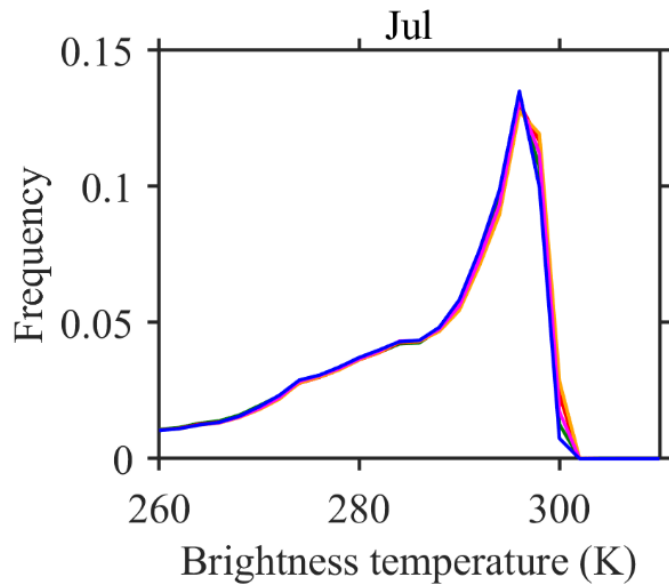
The AGRI brightness temperatures are about 10-20 K higher than the AHI brightness temperatures, in both cloudy and clear-sky areas, regardless over oceans or over land.



Anomalies of AGRI Brightness Temperature at band 8



At 1600, 1700 and 1800 UTC in April and October, the brightness temperature distributions shift to the right with maximum values greater than 310 K.

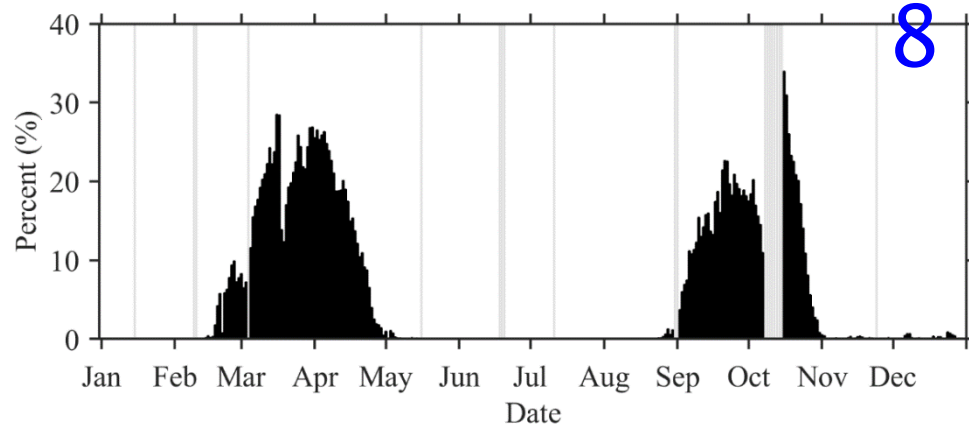


The brightness temperature anomaly at band 8 has a seasonal dependence during midnight from 0000 to 0200 local solar time

— 15 — 16 — 17 — 18 — 19 UTC

Anomalies of AGRI Brightness Temperature at band

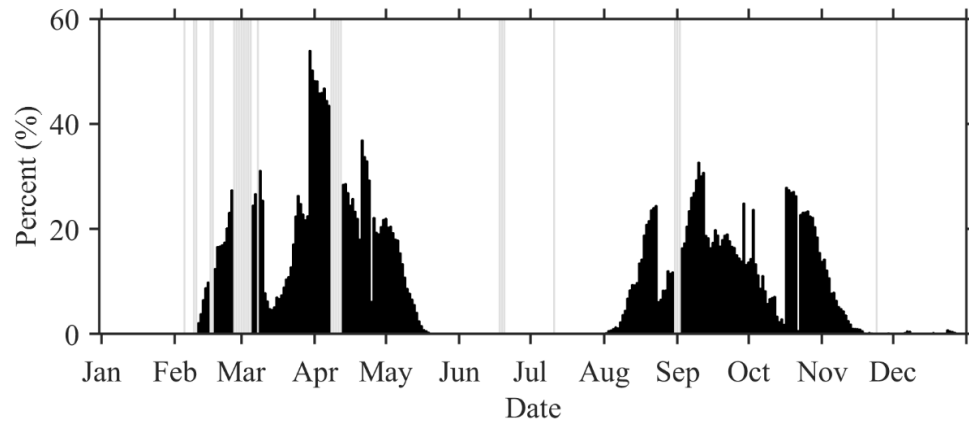
1600 UTC



■ Percentage: number of Tb greater than 300 K / total number of Tb

The anomalies at 1600, 1700 and 1800 UTC hours occurred during the 1-2 month period before and after the vernal or autumnal equinoxes.

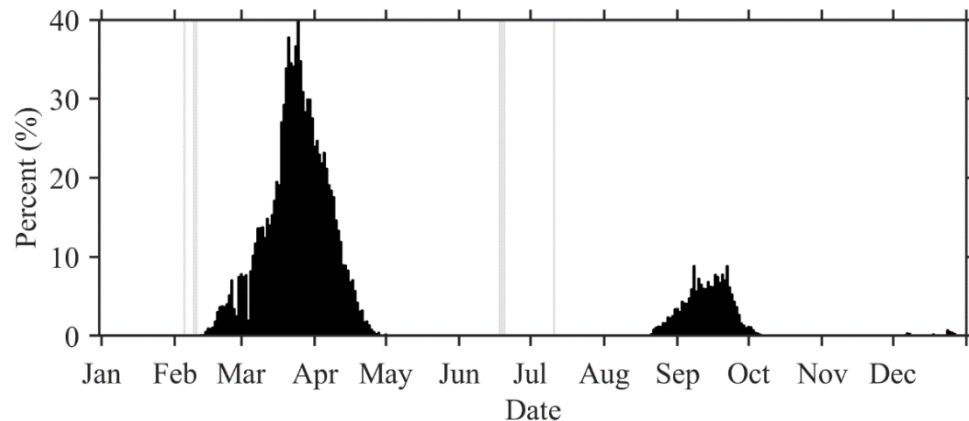
1700 UTC



At 1700 UTC the anomalies last longer than those at 1600 and 1800 UTC hours,

➤ all band data at the hours when the band-8 observations had anomalies are excluded from our statistics.

1800 UTC



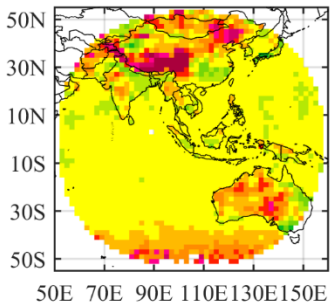
One possible reason is the contamination of 3.75- μm band by stray light at midnight.

Spatial Distributions of AGRI Biases

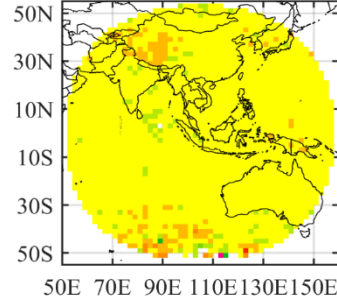
- O-B is calculated with either ERA5 or FNL at 00, 06, 12, 18 UTC as inputs to ARMS.
- The biases over ocean are relatively homogeneous, with an amplitude being less than 1 K.
- The biases over land are heterogeneous, especially for the surface-sensitive bands

O-B^{ERA5}

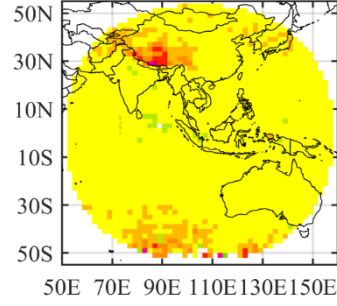
Band 8



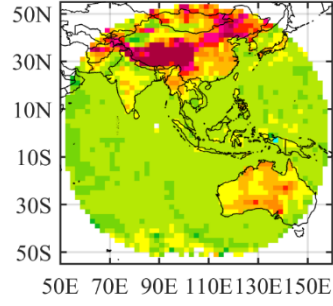
Band 9



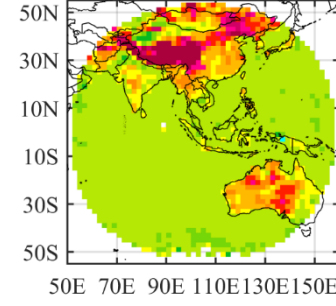
Band 10



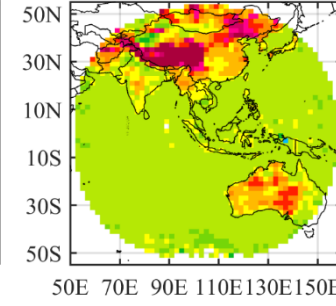
Band 11



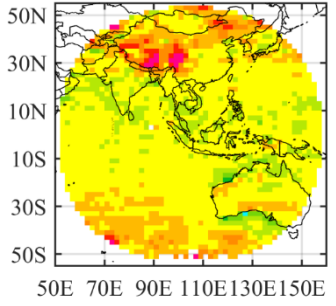
Band 12



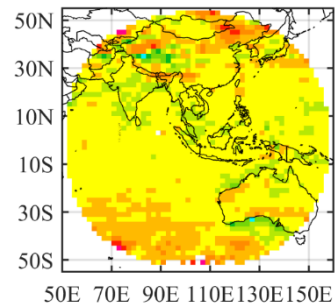
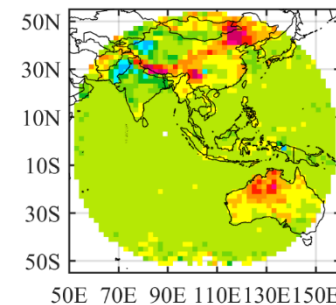
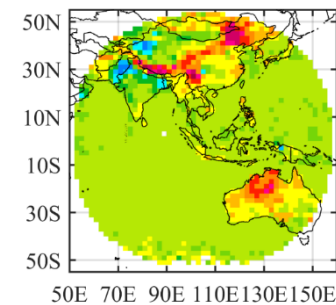
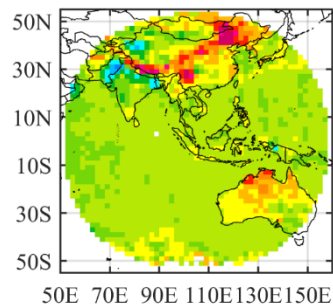
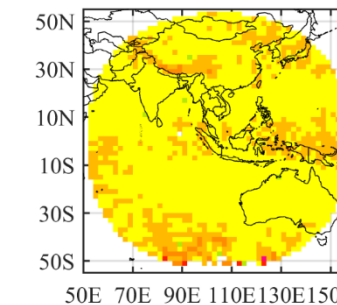
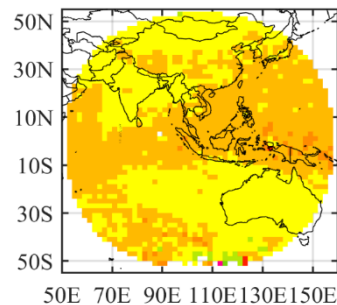
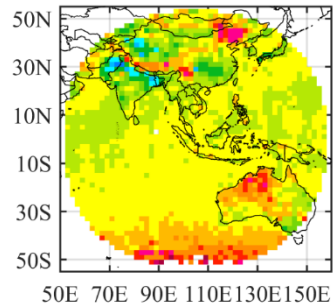
Band 13



Band 14

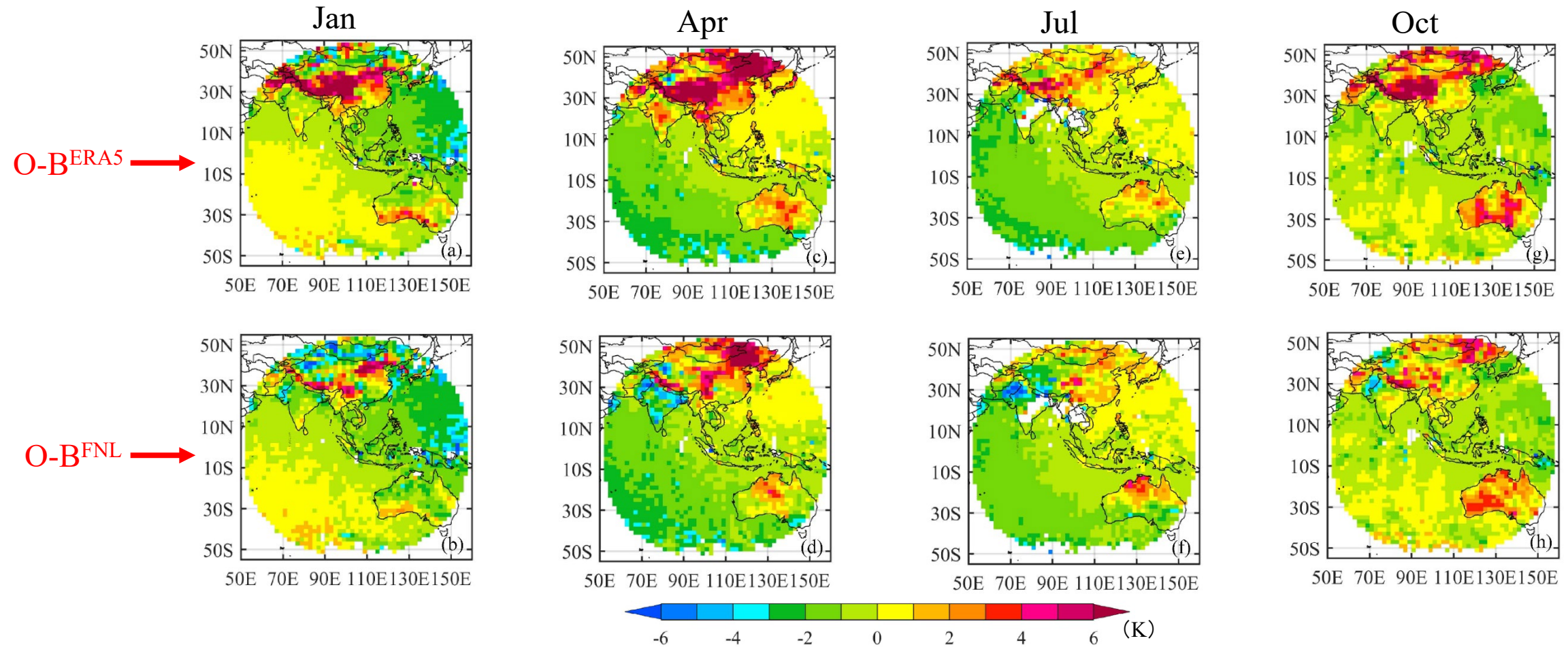


O-B^{FNL}



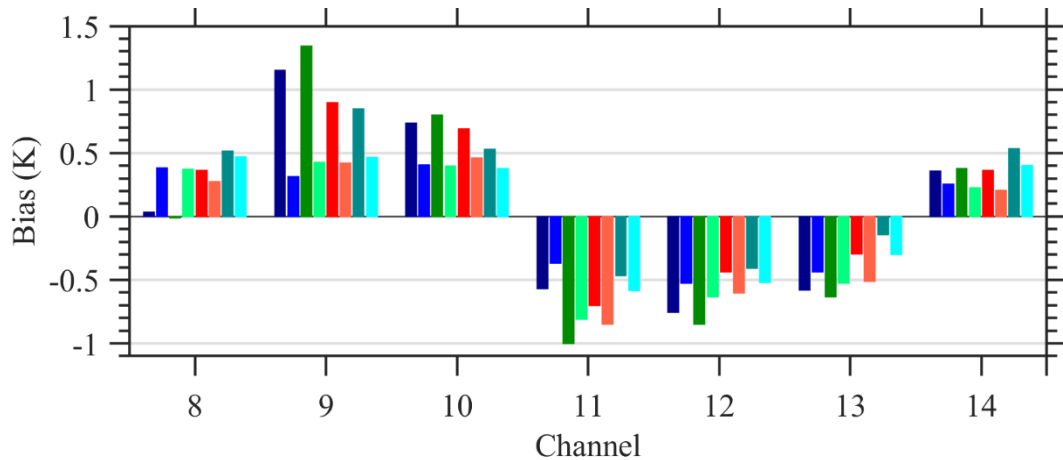
Seasonal Variations of O-B at Band 11

- In April and July, biases show a negative spatial signature in the southwest (Indian Ocean) and a positive one in the northeast (western North Pacific) over the full disk of AGRI, while the opposite characteristics in January and October.
- Bands 12 and 13 have similar characteristics (not show).

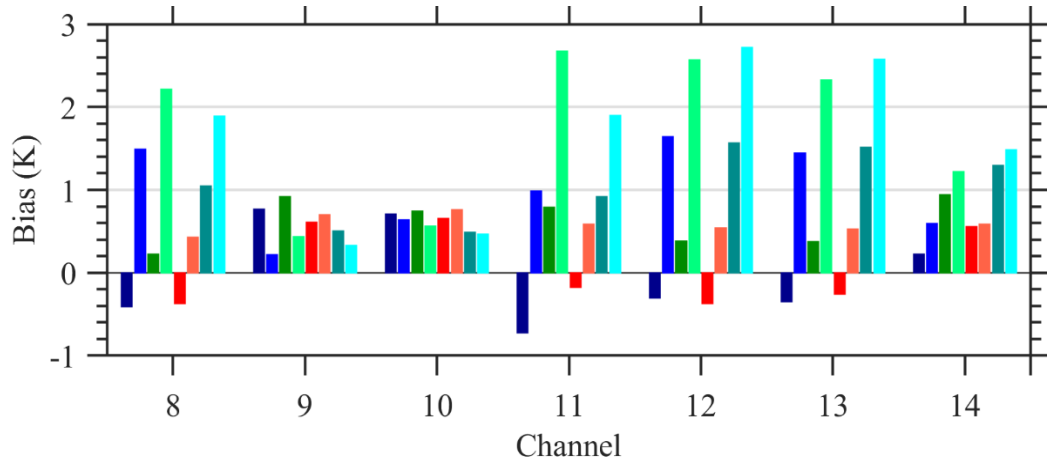


Mean Biases of AGRI

Over ocean



Over land

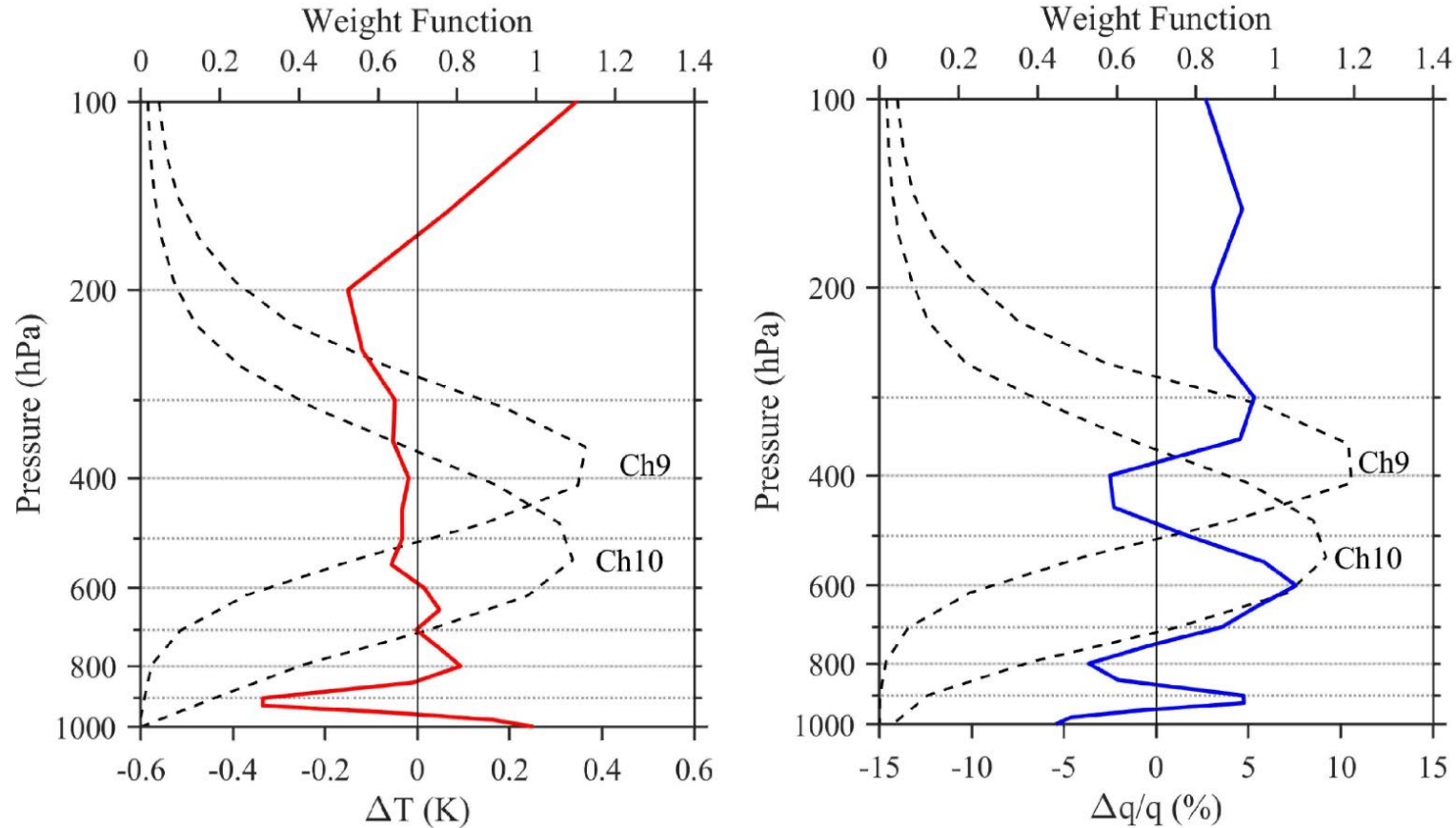


Mean biases (μ) and standard deviations (σ) calculated in Jan., Apr., Jul. and Oct., 2019.

Channel No.	Ocean				Land			
	ERA5		FNL		ERA5		FNL	
	μ (K)	σ (K)	μ (K)	σ (K)	μ (K)	σ (K)	μ (K)	σ (K)
8	0.37	0.92	0.22	1.00	0.64	4.60	-0.64	4.73
9	0.40	0.97	1.06	1.20	0.38	1.47	0.68	1.47
10	0.41	0.94	0.69	1.04	0.59	1.65	0.63	1.56
11	-0.66	1.25	-0.69	1.25	1.18	4.65	-0.05	4.52
12	-0.57	1.13	-0.61	1.16	1.28	5.18	-0.14	5.08
13	-0.45	1.23	-0.41	1.24	1.23	5.01	-0.16	4.87
14	0.27	1.32	0.41	1.32	0.59	2.61	0.36	2.57

- 0.7~1.1 K bias for all seven infrared bands over ocean and three absorption bands over land.
- -0.6~1.3 K bias for four surface-sensitive bands over land.
- The $O-B^{FNL}$ biases are smaller than $O-B^{ERA5}$ over land.
- The standard deviations for $O-B^{ERA5}$ and $O-B^{FNL}$ statistics over land are greater than over ocean.
- For two water vapor bands 9 and 10, the biases of $O-B^{FNL}$ are significantly larger than those of $O-B^{ERA5}$.

Temperature and Humidity Profile Differences between FNL and ERA5 Data

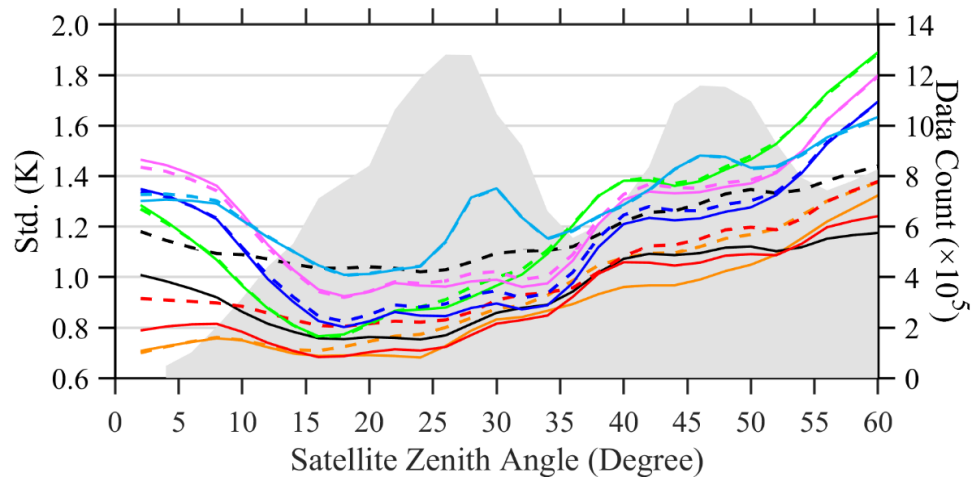
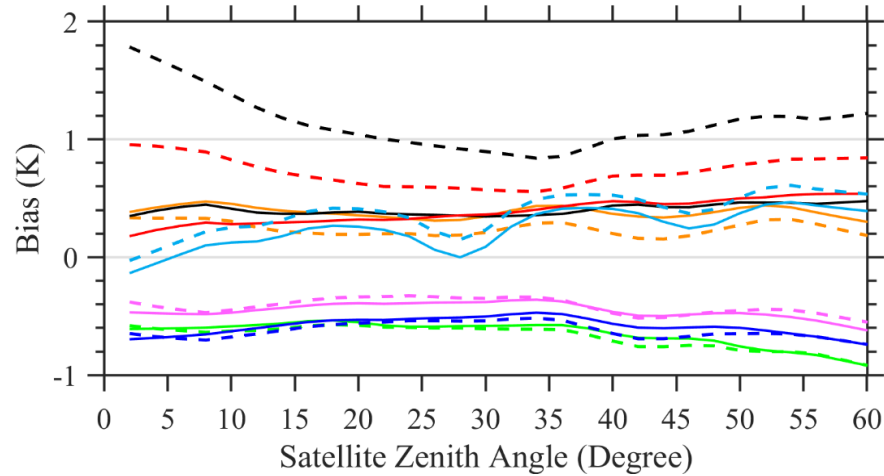


- FNL analysis averaged at 00, 06, 12 and 18 UTC are wetter at 300 hPa and 600 hPa, but drier at 450 hPa and colder above 600 hPa pressure level than the ERA5 reanalysis.
- A deep wetter layer extending from 250 to nearly 400 hPa is right above the weighting function peak level of AGRI band 9.
- A colder layer from 200 to 600 hPa coincides with the weighting function peak levels of two water vapor bands.

Dependence of Bias on Satellite Zenith Angle

Data: January, April, July and October, 2019, over ocean

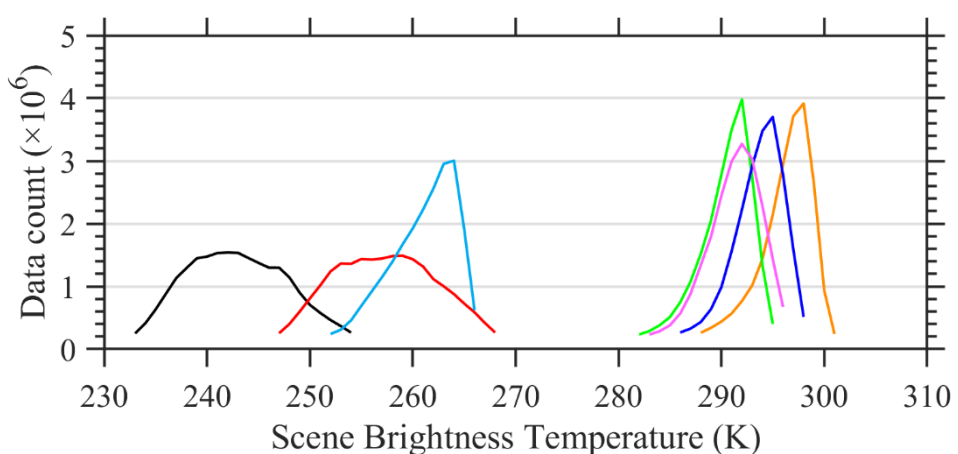
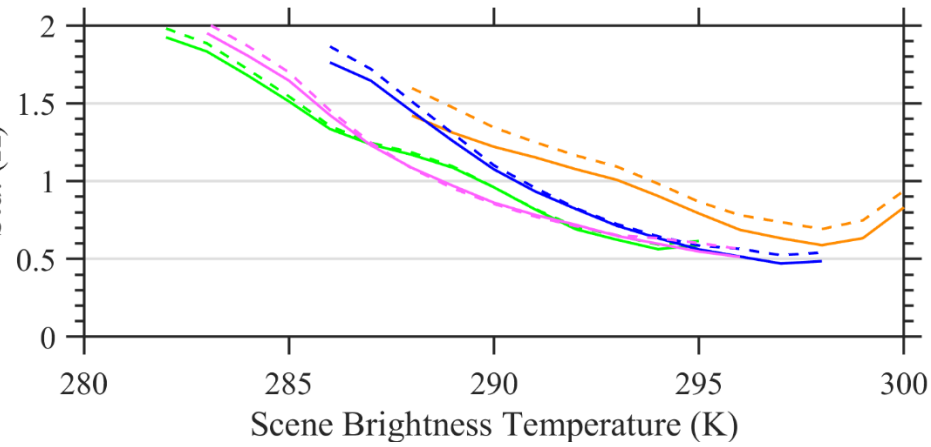
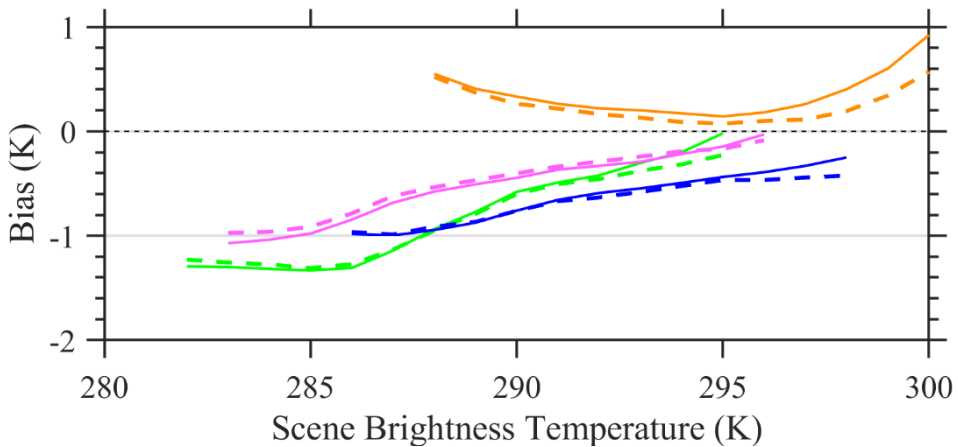
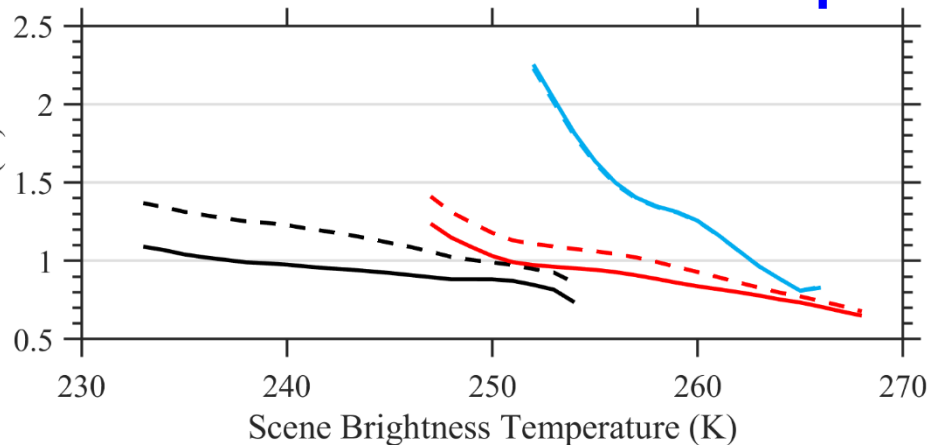
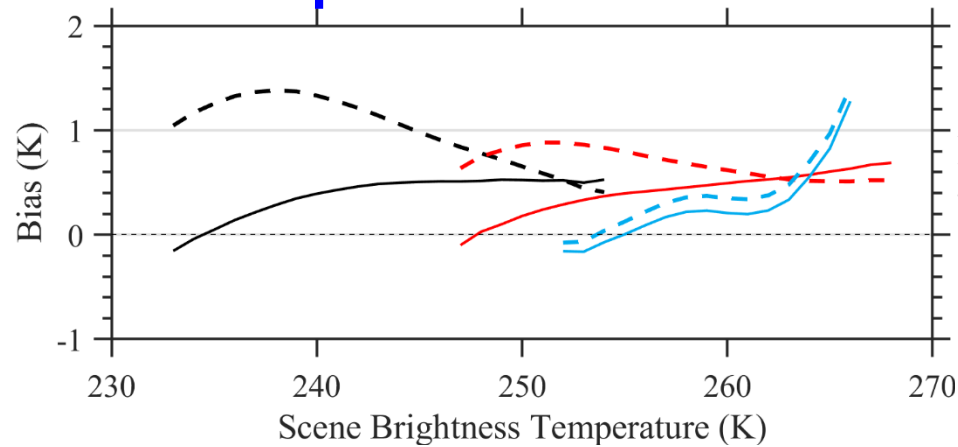
Solid lines: O-B^{ERA5}
Dashed lines: O-B^{FNL}



— Ch8 — Ch9 — Ch10 — Ch11 — Ch12 — Ch13 — Ch14

- No obvious dependence on satellite zenith angle for O-B^{ERA5} biases at bands 8, 9 and 10.
- O-B^{FNL} at bands 9, 10 and 14 show a strong dependence on satellite zenith angle.
- For surface-sensitive bands 11, 12 and 13, both O-B^{ERA5} and O-B^{FNL} biases do not show obvious dependence on satellite zenith angle.
- The standard deviations of IR bands 8-14 vary with the data counts and satellite zenith angle.

Dependence of Bias on Scene Temperature



— Ch8 — Ch9 — Ch10 — Ch11 — Ch12 — Ch13 — Ch14
 Solid lines: O-B^{ERA5}
 Dashed lines: O-B^{FNL}

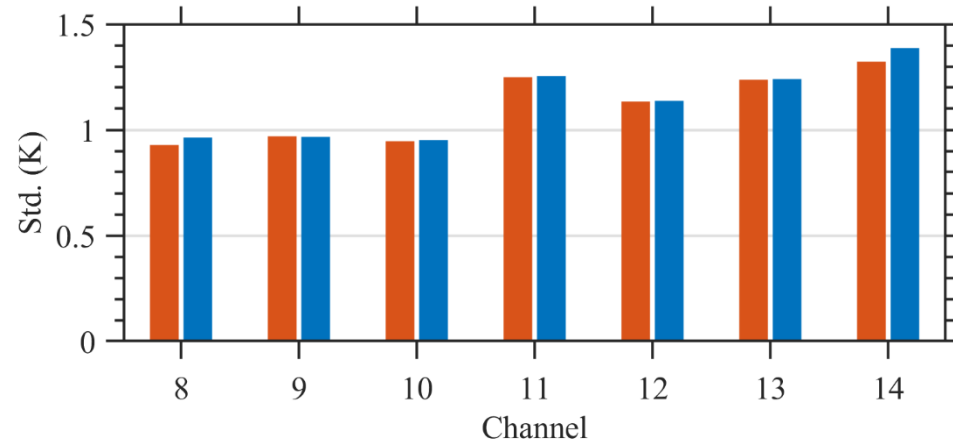
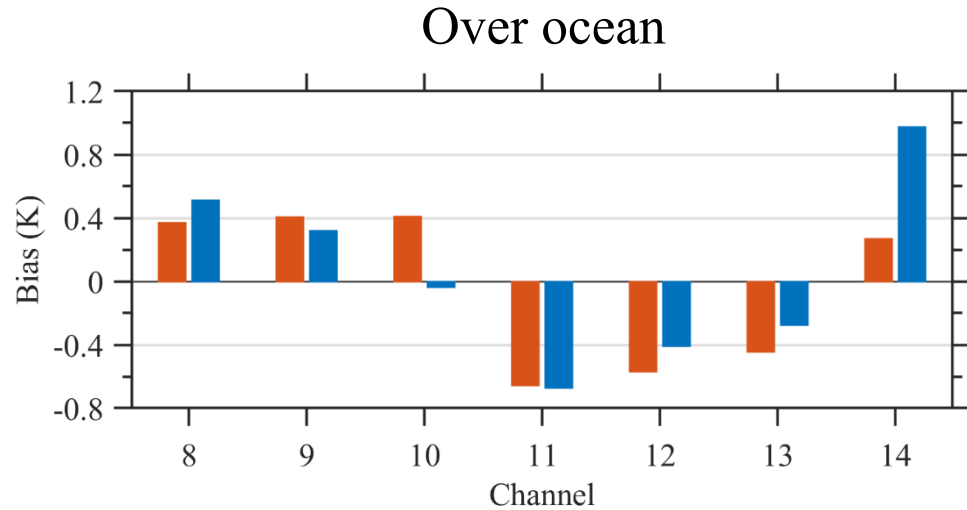
- Obvious scene-temperature dependences of the O-B biases.
- Significant differences exit at bands 9 and 10 in the characteristics of the O-B^{ERA5} and O-B^{FNL} biases with brightness temperature.

outline

- Description of FengYun-4A/AGRI and ARMS
- Data and Method
- AGRI Bias Characteristics
- **Simulation Difference between ARMS and RTTOV**
- Conclusions

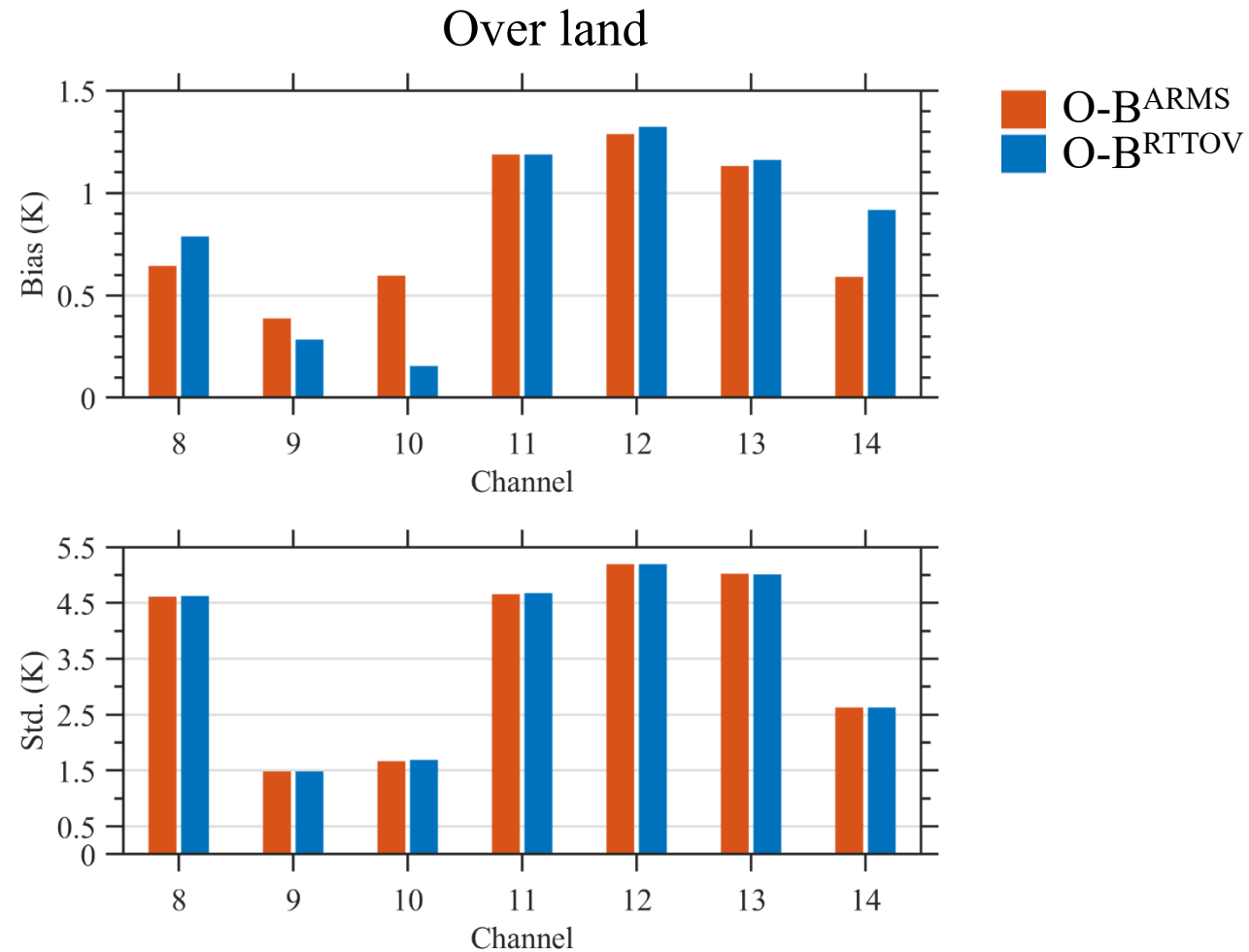
Comparison of $O-B^{ARMS}$ and $O-B^{RTTOV}$

■ $O-B^{ARMS}$
■ $O-B^{RTTOV}$



- the discrepancies of O-B results between two models at AGRI surface-sensitive bands 11-13 are negligible, with a magnitude less than 0.2 K
- $O-B^{ARMS}$ of bands 8 and 14 are smaller than those of $O-B^{RTTOV}$.
- $O-B^{ARMS}$ of water-vapor bands 9 and 10 are larger than $O-B^{RTTOV}$.
- Little difference in the standard deviation of $O-B^{ARMS}$ and $O-B^{RTTOV}$

Comparison of $O-B^{ARMS}$ and $O-B^{RTTOV}$



- Characteristics over land are similar to that over ocean.

Conclusions

- ❑ Brightness temperature anomalies in band 8 are found around the midnight before and after the vernal and autumnal equinoxes.
- ❑ The new developed ARMS model is utilized to characterize biases of the AGRI seven 4 km-resolution infrared bands. The AGRI infrared band bias characteristics are seasonally variable, satellite zenith angle dependent and scene temperature dependent.
- ❑ ARMS shows a great capability to simulate the infrared radiance after a comparison with RTTOV. It will play an important role for future applications of satellite data in numerical weather prediction, retrieval of atmospheric parameters and evaluation of calibration accuracy.